

# Detection and Quantization Technique of Optical Distributed Acoustic Coupling Based on $\varphi$ -OTDR

ZHANG Yang<sup>1</sup> (张洋), XU Hongxuan<sup>1,2</sup> (徐弘萱), ZHU Xianxun<sup>1</sup> (朱贤训),  
ZHAO Zhiyang<sup>1</sup> (赵之阳), ZUO Jiancun<sup>1\*</sup> (左健存)

(1. School of Computer and Information Engineering, Shanghai Polytechnic University, Shanghai 201209, China;  
2. Merchant Marine College, Shanghai Maritime University, Shanghai 201306, China)

© Shanghai Jiao Tong University and Springer-Verlag GmbH Germany, part of Springer Nature 2020

**Abstract:** The detection of multiple acoustic disturbances by optical fiber is a hot research topic in the field of optical fiber sensing. This paper considers adopting an optical distributed acoustic sensing (DAS) system to detect multiple acoustic disturbances, proposes a new approach to processing the DAS signal based on time-space average in frequency domain, and overcomes the randomness of DAS time domain signal. Finally, it obtains a functional model of single-frequency (50—1 000 Hz) sound pressure level and DAS signal intensity, and also the cut-off frequency of acoustic disturbance is detected by DAS system.

**Key words:** distributed acoustic sensing (DAS), sound pressure level, time-space average, quantitative analysis  
**CLC number:** TP 212      **Document code:** A

## 0 Introduction

Optical fiber sensors<sup>[1-4]</sup> have the advantages of no radiation interference, strong anti-electromagnetic interference and high measurement sensitivity. They are widely used in structural monitoring, acoustic wave detection, aerospace and many other fields. Cole et al.<sup>[5]</sup> suggested that sounds can be detected by fiber optics, followed by the use of Mach-Zehnder interferometer (MZI) to detect the acoustically induced phase disturbances in fiber. Kurmer et al.<sup>[6]</sup> used a Sagnac interferometer to detect a single acoustic disturbance on a sensing fiber, but could not detect multiple acoustic perturbations. Taylor and Lee<sup>[7]</sup> used a variation of backscattered coherent Rayleigh noise (CRN) generated by acoustic interference to detect multiple perturbations. This technique enables frequency detection and sound source localization, but cannot quantify the magnitude of the disturbance. Masoudi et al.<sup>[8]</sup> initially studied the relationship between acoustic perturbations and fiber strains. The distributed acoustic sensing (DAS) system has the advantages of multi-point detection and accurate positioning. Golacki et al.<sup>[9]</sup> verified that the DAS system<sup>[10]</sup> can detect the disturbance of sound waves to the fiber in the reverberation room. Stajanca et al.<sup>[11]</sup> proposed a DAS signal processing

method based on frequency-domain time-average, but did not quantify the DAS signal and the sound pressure level.

This paper considers using the DAS system to detect multiple acoustic disturbances and adopts a time-space average method in frequency domain to make the quantitative analysis. The basic principle of the DAS system for detecting acoustic disturbances is detailed in Section 1, followed by a description of experimental layout in Section 2. The experimental results are given in Section 3, it also analyzes and discusses the results there. Finally, the conclusions are summarized.

## 1 Principle of DAS System

The DAS system is based on a coherent Rayleigh scattering. The detection principle is shown in Fig. 1, where PD is the photoelectric detector, ADC is the analog to digital converter, and EDFA is the erbium-doped fiber amplifier. The phase-optical time domain reflectometer ( $\varphi$ -OTDR) technology is applied to the DAS system. A highly coherent light pulse acts as a probe light entering the sensor fiber through the circulator. When the intrusion occurs, the refractive index of the fiber changes, causing the phase change of the back-scattered Rayleigh scattered light. Due to the interference, the back-to-Rayleigh scattered light intensity changes accordingly, and the detector detects the reflection from different positions of the fiber and extracts a weak perturbation signal<sup>[12-13]</sup>.

In the single-mode fiber, according to the one-

---

**Received date:** 2019-05-06

**Foundation item:** the Graduate Program Foundation of Shanghai Polytechnic University (No. EGD18YJ0045)

**\*E-mail:** jcزو@sspu.edu.cn

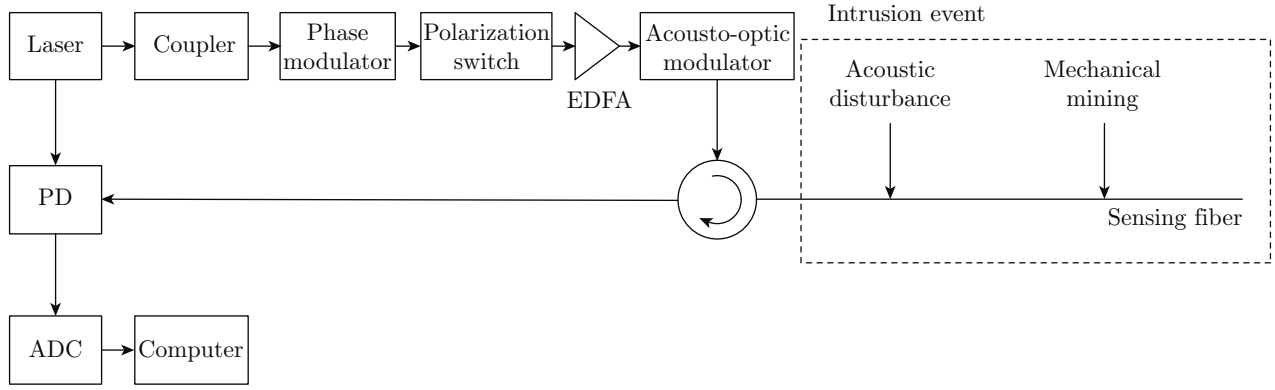


Fig. 1 DAS system detection principle

dimensional impulse response model of the fiber backward Rayleigh scattering<sup>[14]</sup>, the incident laser is a rectangular pulse, the fiber is injected at time  $t = 0$ , and the back-range Rayleigh scattering wave amplitude can be obtained<sup>[14]</sup>:

$$e(t) = \sum_{i=1}^N a_i \exp\left(-a \frac{c\tau_i}{n}\right) \exp\left(j2\pi F(t - \tau_i)\right) \text{rect}\left(\frac{t - \tau_i}{w}\right), \quad (1)$$

where,  $i$  is the number of scattering centers;  $N$  is the number of scattering centers;  $a_i$  is the amplitude of the  $i$ -th scattering wave;  $a$  is the attenuation coefficient of the fiber;  $c$  is the speed of light in vacuum;  $n$  is the refractive index of the fiber;  $\tau_i = \frac{2nl_i}{c}$  is the time delay of the  $i$ -th scattering wave,  $l_i$  is the length of the fiber from the  $i$ -th scattering center to the input;  $F$  is the frequency;  $\text{rect}(\cdot)$  is the rectangular function;  $w$  is the pulse width.

The modulation frequency of acousto-optic modulator (AOM) is  $f$ . After continuously injecting  $m$  pulses, the input will obtain a continuous backward Rayleigh scattering wave with a period of  $T = 1/f$ , and its amplitude is expressed as

$$e(t') = \sum_{k=1}^m \sum_{i=1}^N a_i \exp\left(-a \frac{c\tau_i}{n}\right) \exp\left(j2\pi F\left(t' - \frac{k}{f} - \tau_i\right)\right) \text{rect}\left(\frac{t' - \frac{k}{f} - \tau_i}{w}\right), \quad (2)$$

where,  $k$  is the number of pulses.

Then the backward Rayleigh scattered light power is

$$p(t') = |e(t')|^2 = p_a(t') + p_b(t'), \quad (3)$$

where,  $p_a(t')$  represents the sum of the optical powers of each independent backscatter center for a large number of scattering centers;  $p_b(t')$  is caused by interference

and has a sawtooth ripple. When the sawtooth ripple is generated by  $\cos(2\pi F(\tau_i - \tau_j))$ , the phase difference is

$$\theta_{ij} = \cos(2\pi F(\tau_i - \tau_j)) = 4\pi F n(l_i - l_j). \quad (4)$$

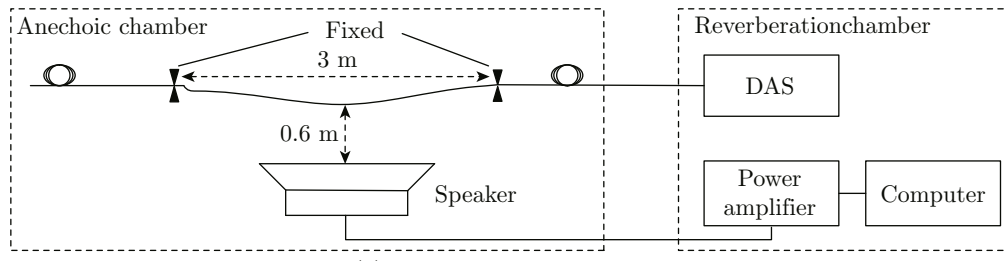
When the optical fiber is disturbed by sound, the phase difference between the two interfering scattered waves changes:  $\theta_{ij} = 4\pi F(n + \Delta n)(l_i - l_j)$ . This results will lead to a change in the backward Rayleigh light intensity  $p_b(t')$ . The detection and the localization of the acoustic disturbance can be achieved by detecting the intensity variation of the back-reverse Rayleigh scattered light signal before and after the disturbance.

## 2 Experimental Arrangement

The experimental scheme is shown in Fig. 2. The DAS system is placed in the reverberation chamber. As shown in Fig. 2(b), the anechoic chamber has a net volume of 1 200 m<sup>3</sup>. The 6 sides are fully covered with sound-absorbing cusps. There is only a direct sound in the room and no reflection of sound waves. The influence of environmental background noise on the experiment is reduced. The laser light from a narrow linewidth laser operating at 1 550 nm in a DAS system is modulated to produce an optical pulse with a pulse width of 50 ns and a repetition rate of 20 kHz into the sensing fiber.

A 1 km sensing fiber of standard mode fiber including a 3 m section where acoustic disturbance is imposed by using a speaker. The speaker is placed under the fiber, and the fiber is kept in a relaxed state. The lowest point of the fiber is 0.6 m from the speaker.

The background noise level of the muffler room is lower than 40 dB, the frequency is lower than 100 Hz, the sound pressure level of the speaker output sound wave is 60–85 dB, and the frequency range is 50–5 000 Hz. In order to improve the sensitivity and the linear stability of the system<sup>[9]</sup>, the detection time of the DAS is 3 min.



(a) Experimental arrangement



(b) Anechoic chamber



(c) Acoustic disturbance device



(d) DAS detection system

Fig. 2 Experimental schematic and experimental photos

### 3 Results and Analysis

The 3D diagram of Fig. 3 shows the fast fourier transformation (FFT) of the DAS output for a 50 dB sound pressure level at a frequency of 200 Hz. The frequency, the location, and the amplitude of the peak in this 3D diagram are accurately indicating those of the speaker. The DAS signal with a frequency between 20 and 1 000 Hz is accumulated and then the space average is performed:

$$D_P(t) = \frac{1}{b_2 - b_1} \sum_{p=b_1}^{b_2} D(t), \quad (5)$$

where,  $b_1, b_2$  are the starting and end positions of the sensing fiber in response to the acoustic disturbance;

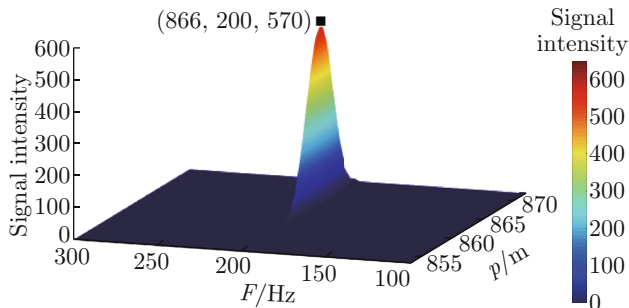


Fig. 3 3D plot of FFT of the DAS output for the data points at 866 m

$p$  is the position of the sensing fiber in response to the acoustic disturbance;  $D(t)$  is the DAS time domain signal.

The fiber contains all the energy of the post-excited coupling by accumulating. Because the experiment is performed in the muffler chamber, this energy is directly coupled into the fiber without any reflection.

As shown in Fig. 4, the DAS system is capable of detecting disturbance of acoustic disturbance with different sound pressure levels (60—85 dB) and different frequency (50—1 000 Hz) on the fiber. However, the randomness of the time domain signal is obvious, and the long-term cumulative average can reduce the influence of randomness. In order to verify that the randomness is reduced, the DAS signal is processed by time-average on the basis of space-average ( $D_{pt}(p, t)$ ), and the accumulated time is 3 min.

In order to reduce the influence of the DAS signal randomness in the time domain on the quantizing sound pressure level and the DAS signal intensity, the accumulated DAS signals are processed by time-average based on space-average.

$$D_{pt}(p, t) = \frac{1}{n} \sum_{t=0}^n D_P(t). \quad (6)$$

The relationship between  $20 \lg D_{pt}(p, t)$  (denoted as  $D_{pt}(s)$ ) and sound pressure level (denoted as  $s$ ) at different frequencies is shown in Fig. 5.

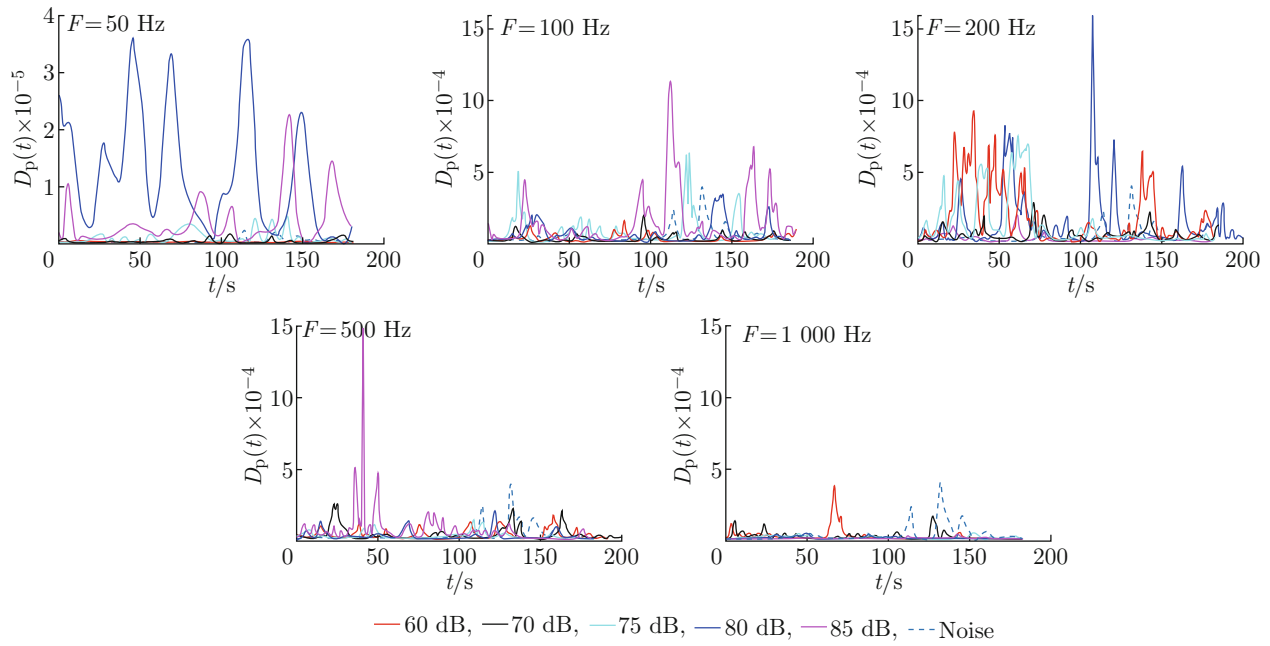


Fig. 4 2D plot of time domain of the DAS output for the data points between 865 and 867 m

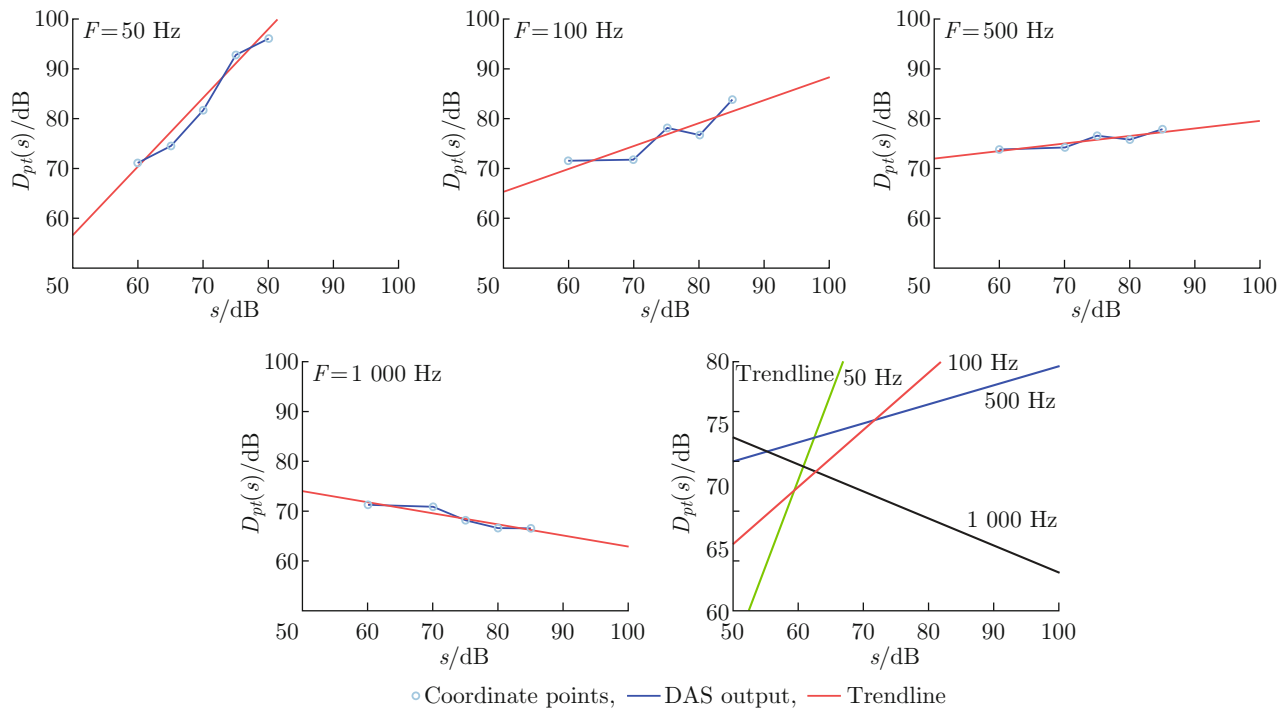


Fig. 5 Relationship between  $s$  and  $D_{pt}(s)$

As shown in Fig. 5, the DAS signal is correlated with  $s$  and  $F$ . The functional model of  $s$  and  $D_{pt}(s)$  is obtained.

$$D_{pt}(s) = \begin{cases} 1.38s - 12.69, & F = 50 \text{ Hz} \\ 0.46s + 42.28, & F = 100 \text{ Hz} \\ 0.15s + 84.85, & F = 500 \text{ Hz} \\ -0.21s + 64.35, & F = 1000 \text{ Hz} \end{cases} \quad (7)$$

The coefficients of determination (R-square) of Eq. (7) are 0.74, 0.78, 0.88 and 0.82 respectively. A good linear relationship verifies that such data processing is reasonable. The long-term cumulative average can reduce the influence of randomness. In order to verify that the randomness is reduced, the accumulative times of 30, 60, and 180 s were compared. Different accumulative times have different effects on the R-square,

as shown in Table 1. The long-term cumulative average increases the R-square and reduces the influence of randomness.

**Table 1 Comparison of different accumulative times**

Cumulative time/s	R-square			
	50 Hz	100 Hz	500 Hz	1 000 Hz
30	0.55	0.61	0.52	0.75
60	0.57	0.71	0.76	0.78
180	0.74	0.78	0.88	0.82

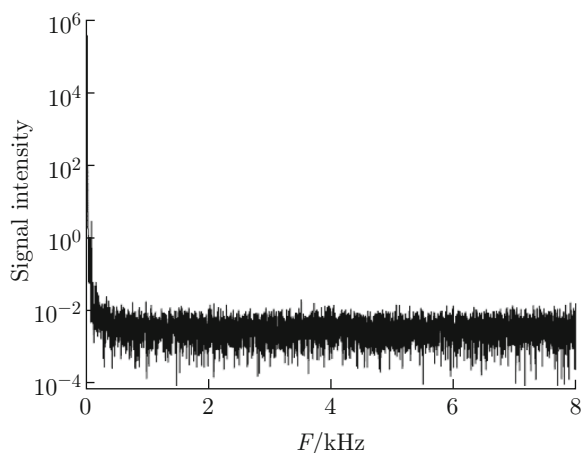
As shown in Table 2, the paper compares with similar studies. In order to meet the practical application, this

paper improves the experimental environment and the fiber laying method, and proposes a new approach to processing the DAS signal based on time-space average in frequency domain. Finally, it got the quantitative result.

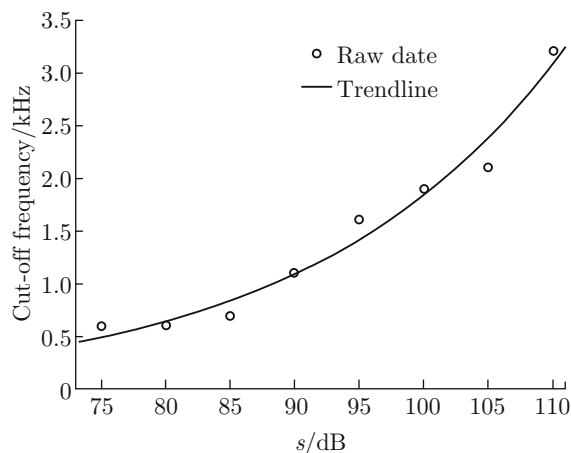
The fiber is disturbed by white noise of different sound pressure levels. The DAS signal spectrum is shown in Fig. 6(a) when  $s = 85$  dB. Low frequency coupling coefficient is much larger than high frequency. The high frequency part and the low frequency part are respectively made tangent, and the cutoff frequency corresponding to different sound pressure levels can be obtained. As shown in Fig. 6(b), cut-off frequency of DAS responses to different sound pressure levels. The trendline divides Fig. 6(b) into two regions including the signal region and the no signal region.

**Table 2 Comparative analysis with similar studies**

Experimental environment	Fiber arrangement	Data collection	Data processing	Spatial and frequency resolution	Relationship between sound pressure level and sensing signal intensity
General laboratory	Bare fiber is laid on polyethylene sheet	A point on the fiber	FFT	1 m, 100 Hz	No quantification
Reverberation room	Bare fiber overhead laying	4 m fiber length	FFT and space average	1 m, 1 Hz	No quantification
Anechoic chamber	Bare fiber overhead laying	3 m fiber length	FFT and time-space average	1 m, 1 Hz	Quantification



(a) DAS signal spectrum with  $s = 85$  dB



(b) Cut-off frequency of DAS responses

Fig. 6 Frequency response of DAS

## 4 Conclusion

The DAS system demonstrated in this paper is capable of quantitatively measuring single-frequency (50—1 000 Hz) multiple acoustic disturbances. DAS signal

intensity varies with space, time, and acoustic frequency. The randomness of time domain signals is overcome by using the approach to processing the DAS signal based on time-space average in frequency domain. A functional model of sound pressure level of single-

frequency and DAS signal intensity is established. Due to the unique nature of the coupling of fiber and sound, the cut-off frequency of the DAS system to detect the acoustic disturbance is obtained. This paper provides the basis for the DAS system to detect and warn a gas pipeline leakage.

## References

- [1] SHANG Y, WANG C, WANG C, et al. Distributed vibration sensing of perimeter security based on space difference of Rayleigh backscattering [J]. *Infrared and Laser Engineering*, 2018, **47**(5): 0522001.
- [2] ZHOU D, DONG Y, WANG B, et al. Slope-assisted BOTDA based on vector SBS and frequency-agile technique for wide-strain-range dynamic measurements [J]. *Optics Express*, 2017, **25**(3): 1889-1902.
- [3] HANG L J, HE C F, WU B, et al. Research on novel distributed optical fiber pipeline leakage detection technology and location method [J]. *Acta Optica Sinica*, 2008, **28**(1): 123-127 (in Chinese).
- [4] ZHANG Y, CAO Y Y, ZHU Y S, et al. Distributed Brillouin scattering optical fiber strain sensor technology [C]//*3rd Advanced Information Technology, Electronic and Automation Control Conference*. Chongqing, China: IEEE, 2018: 731-737.
- [5] COLE J H, JOHNSON R L, BHUTA P G. Fiber-optic detection of sound [J]. *The Journal of the Acoustical Society of America*, 1977, **62**(5): 1136-1138.
- [6] KURMER J P, KINGSLEY S A, LAUDO J S, et al. Distributed fiber optic acoustic sensor for leak detection [C]//*Distributed and Multiplexed Fiber Optic Sensors*. Boston, MA, USA: SPIE, 1992: 117-128.
- [7] TAYLOR H F, LEE C E. Apparatus and method for fiber optic intrusion sensing: US5194847 [P]. 1993-03-16.
- [8] MASOUDI A, BELAL M, NEWSON T P. Distributed optical fibre audible frequency sensor [C]//*23rd International Conference on Optical Fibre Sensors*. Santander, Spain: SPIE, 2014: 91573T.
- [9] GOLACKI P, MASOUDI A, HOLLAND K R, et al. Distributed optical fibre acoustic sensors — future applications in audio and acoustics engineering [C]//*Acoustics 2016*. Kenilworth, UK: Institute of Acoustics, 2016.
- [10] TU Q C, WEI B, ZHANG Z Y, et al. OTDR-type distributed optical fiber Sensors and application of oil and gas pipelines online monitoring [J]. *Pipeline Technology and Equipment*, 2015(3): 28-31 (in Chinese).
- [11] STAJANCA P, CHRUSCICKI S, HOMANN T, et al. Detection of leak-induced pipeline vibrations using fiber: Optic distributed acoustic sensing [J]. *Sensors*, 2018, **18**(9): 2841.
- [12] JUŠKAITIS R, MAMEDOV A M, POTAPOV V T, et al. Interferometry with Rayleigh backscattering in a single-mode optical fiber [J]. *Optics Letters*, 1994, **19**(3): 225-227.
- [13] RATHOD R, PECHSTEDT R D, JACKSON D A, et al. Distributed temperature-change sensor based on Rayleigh backscattering in an optical fiber [J]. *Optics Letters*, 1994, **19**(8): 593-595.
- [14] LÜ L, XING Y W. Investigation on Rayleigh scattering waveform in phase optical time domain reflectometer [J]. *ACTA Optical Sinica*, 2011, **31**(8): 0819001 (in Chinese).